

Coupling disorder in a population of swarmalators

Hyunsuk Hong,^{1,2} Kangmo Yeo,¹ and Hyun Keun Lee³

¹*Department of Physics, Jeonbuk National University, Jeonju 54896, Korea*

²*Research Institute of Physics and Chemistry, Jeonbuk National University, Jeonju 54896, Korea*

³*Department of Physics, Sungkyunkwan University, Suwon 16419, Korea*

(Dated: September 1, 2021)

We consider a population of two-dimensional oscillators with random couplings, and explore the collective states. The coupling strength between oscillators is randomly quenched with two values one of which is positive while the other negative, and the oscillators can spatially *move* depending on the state variables for phase and position. We found that the system shows the phase transition from the incoherent state to the fully synchronized one at a proper ratio of the number of positive couplings to the total. The threshold is numerically measured, and analytically predicted by the linear stability analysis of the fully synchronized state. It is found that the random couplings induces the long-term state patterns appearing for constant strength. The oscillators move to the places where the randomly quenched couplings work as if annealed. We further observe that the system with mixed randomnesses for quenched couplings shows the combination of the deformed patterns understandable with each annealed averages.

PACS numbers: 05.45.-a, 89.65.-s

I. INTRODUCTION

In recent studies [1, 2], oscillators that sync and swarm, called as *swarmalators*, have been considered, and interesting long-term states have been found. The swarmalators can move in the space under the correlated dynamics of the phase and space variables of each oscillator. The *mobile* feature of the oscillators is found to induce non-stationary states such as the active-phase wave state and the splintered phase wave one. The collective property of finite number of swarmalators is studied [3], the implementation in robots is tried as an application [4], and various steady states by finite interaction-distance is reported [5]. In the theoretical and practical interest, the swarmalator model has been studied in the various fields ranging from science to engineering [6–11].

In the study of swarmalators, the interesting incoherent states are usually the consequence of negative-definite coupling strength in phase dynamics (positive-definite case is also in [2] where noise is added). On the other hand, the coupling characteristic among the constituents of many systems is rather complex and not so simple. For example, the interaction among the neurons in the neural network systems is given by the mixture with positive and negative ones [12, 13], in general. As another example, Japanese frogs' calling behavior can be understood by considering the mixture of positive and negative interaction with each other [14]. Probably, the spin glass [15, 16], to which the various interesting properties of condensed matter is attributed, can be the representative example for the non-definite sign of the couplings. Considering those features in nature, the mixed coupling with positive and negative strength deserves to be considered for understanding the collective behavior of the real systems, which motivates the present study.

In this paper, we consider a population of the oscillators that can sync and swarm, governed by the random

interaction in the phase dynamics. We explore how the coupling-disorder affects the long-term states in the system. In particular, we pay attention to the possibility of the phase transition [17] in the system, and focus on whether the patterns observed in the absence of coupling disorder still appear. The effective annealing of the randomly quenched coupling strengths to their average is suggested in the mobility of swarmalators to understand the numerical results. Phase transition to fully synchronized phase, reproducibility of the phases known in the original model of no coupling disorder, and mixture of deformed long-term states by coupling disorders are explained in the viewpoint of the annealed couplings.

This paper is organized as follows: Section II introduces the model of coupled swarmalators with random couplings, and Sec. III shows the collective behavior and the phase transition in the system. In Sec. IV we derive the threshold of the transition by the linear stability analysis of the fully synchronized state. Various long-term states including the nonstationary ones are shown in Sec. V, and the system with couplings of more than one quenched randomness are understood as the combination of annealed-coupling systems in Sec. VI. A brief summary is given in Sec. VII.

II. MODEL

The generalized model of N -coupled oscillators that we consider here is given by

$$\frac{d\theta_i}{dt} = \frac{1}{N} \sum_{j \neq i} F(r_{ij}) K_{ij} \sin(\theta_j - \theta_i), \quad (1)$$

$$\frac{d\mathbf{r}_i}{dt} = \frac{1}{N} \sum_{j \neq i} G(r_{ij}, \theta_{ij}) \quad (2)$$

for $i = 1, \dots, N$, where θ_i and \mathbf{r}_i represent the phase ($0 \leq \theta_i \leq 2\pi$) and the position vector of the i th oscillator, respectively. The $F(r_{ij})$ is a function for the spatial dynamics of the oscillators with $r_{ij} = |\mathbf{r}_{ij}|$ for $\mathbf{r}_{ij} \equiv \mathbf{r}_j - \mathbf{r}_i$, and the $G(r_{ij}, \theta_{ij})$ is a function for spatial dynamics with $\theta_{ij} \equiv \theta_j - \theta_i$. The K_{ij} denotes the random coupling strength between the oscillators i and j , having the symmetric property, $K_{ij} = K_{ji}$. It represents a sort of *bond* coupling between the oscillators, instead of the *site* one (K_i) that affects the oscillator itself. For simplicity, we randomly choose K_{ij} from the two-peaks distribution

$$h(K_{ij}) = p\delta(K_{ij} - K_p) + (1-p)\delta(K_{ij} - K_n), \quad (3)$$

where p is the probability of the positive coupling, and $K_p > 0$ and $K_n < 0$. For convenience, the ratio $Q \equiv -K_n/K_p (> 0)$ has been chosen for the control parameter. With the functions F and G in the model, the phase variable θ and the spatial one r have the correlation, which makes the oscillators can move around in the space. Such correlation in the dynamics of space and phase of the oscillators has been also studied in Ref. [1], where the authors found five long-term states including the two nonstationary ones. Note that the phase coupling in Ref. [1] does not have any disorder, and only a constant coupling ($K_{ij} = K (< 0)$) has been considered, which corresponds to $p = 0$ in Eq. (3). We here consider coupling disorder with more general value p in $0 \leq p \leq 1$, which introduces the positive(ferromagnetic) couplings in the system.

We notice that the special case with $F(r_{ij}) = 1$ and $G(r_{ij}, \theta_{ij}) = 0$ is equivalent to the mean-field XY model [16] with *random* coupling strength, governed by the Hamiltonian $\mathcal{H} = -\frac{1}{2N} \sum_{i \neq j} K_{ij} \cos(\theta_j - \theta_i)$. Equation (1) with $F = 1$ and $G = 0$ leads to the overdamped version of the Hamiltonian dynamics at zero temperature, and interestingly it is found that the first-order phase transition occurs at the same threshold p_c as that we study here [18].

In this paper, we consider $F = 1/r_{ij}$. The function G consists of the attraction and repulsion forces acting on each oscillator, where the force functions are taken as the algebraic ones with a power like r_{ij}^{-a} following the Ref. [1]. The model is then given by

$$\dot{\theta}_i = \frac{1}{N} \sum_{j \neq i} \frac{K_{ij}}{r_{ij}} \sin(\theta_j - \theta_i), \quad (4)$$

$$\dot{\mathbf{r}}_i = \frac{1}{N} \sum_{j \neq i} \left[\frac{\mathbf{r}_{ij}}{r_{ij}} (A + J \cos(\theta_j - \theta_i)) - B \frac{\mathbf{r}_{ij}}{r_{ij}^2} \right], \quad (5)$$

where the A and B are respectively the parameters for the attractive force and repulsive one. Here, we choose $A = B = 1$ for convenience. The J is the parameter which measures how the phase similarity enhances the spatial proximity. For example, positive value of J means *like attracts like*, i.e., the swarmalators tend to be near the other swarmalators with similar phases. On the other

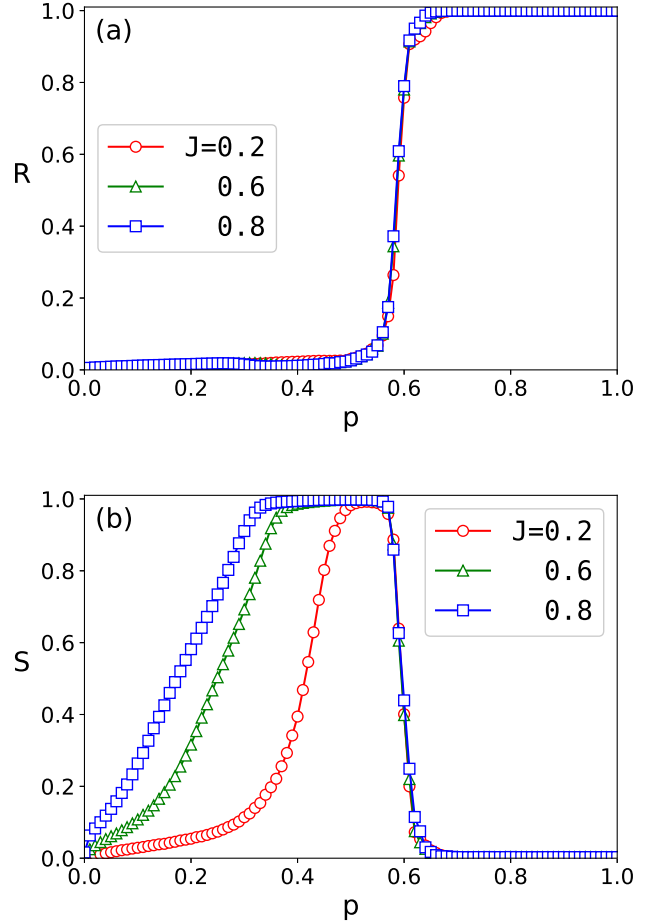


FIG. 1. (Color Online) (a) R is shown as a function of p for various values of J ; (b) S vs. p for various values of J . Parameters: $Q = 1.25$ and $N = 200$.

hand, negative value of J means the opposite case: The swarmalators prefer to be near the others with opposite phases. To keep the attractive force always positive, the values of J are constrained like $-1 \leq J \leq 1$, following the Ref. [1]. The difference from the model of Ref. [1] is the generalization of constant K to pair-dependent K_{ij} . For $K_{ij} > 0$, the swarmalators prefer to have the similar phase, but for $K_{ij} < 0$, the opposite tendency occurs. We are interested in the effect of random K_{ij} in the formation of long-term states.

III. PHASE TRANSITION

To see the collective states in the system and the effects of random coupling on the states we perform the numerical simulations on Eqs. (4) and (5). We first investigate the phase synchronization behavior of the oscillators, by

measuring the complex order parameter defined by [19]

$$Re^{i\Theta} = \frac{1}{N} \sum_{j=1}^N e^{i\theta_j}, \quad (6)$$

where R measures the phase coherence, and the Θ is the mean phase angle of the oscillators. For example, $R = 0$ means the incoherent state where the all oscillators have the random phase $\theta_i \in [0, 2\pi)$, and $R = 1$ is the fully synchronized state where the all have the same one $\theta_j = \theta_s$ for all j 's.

Also, to see the correlation between the phase angle θ_j and the azimuthal one $\phi_j = \tan^{-1}(y_j/x_j)$ for the j th oscillator, which is induced by the mobile feature of the oscillators in the system, we measure another order parameter defined by [1]

$$S_{\pm} e^{i\Psi_{\pm}} = \frac{1}{N} \sum_{j=1}^N e^{i(\phi_j \pm \theta_j)}, \quad (7)$$

where S_{\pm} is the magnitude, and the Ψ_{\pm} is its mean phase, respectively. Here, the order parameter S measures the ‘‘correlation’’ between the spatial information (by the ϕ_j) and the phase one (by the θ_j). The system exhibits ‘‘assortative/commutative’’ correlation between the two depending on the initial conditions, where the S_+ comes from the assortative correlation, and S_- from the commutative correlation, respectively. We choose S by taking the maximum value of S_+ and S_- , i.e., $S = \max(S_{\pm})$ [1].

In order to examine R and S , we basically performed the numerical simulations using the Python or C programs. The total 5×10^4 time steps with the discrete time unit $dt = 0.1$ have been considered, where the first 2.5×10^4 steps were discarded for the equilibrium, and then the time average of the quantities has been done for the later steps. And, the ten samples have been used for the average. Initial phases and positions are, respectively, randomly sampled from the uniform distributions over $[0, 2\pi)$ and $[-1, 1) \times [-1, 1)$.

Figure 1 shows the behavior of R and S as a function of p for various values of J . The value of $Q = 1.25$ is chosen, where $K_p = 1$ and $K_n = -1.25$ have been chosen for convenience. We find that the system shows the phase transition behavior from the incoherent state ($R = 0$) to the fully synchronized one ($R = 1$) at a finite value of p , i.e., ($p_c \sim 0.6$). Interestingly, we find that the behavior of R and its threshold p_c do not depend on J , which can be easily understood by the absence of J in the phase dynamics given by Eq. (4). On the other hand, the behavior of S is different from that of R as shown in Fig. 1: In the regime of fully synchronized state ($R = 1$) for $p > p_c$, the order parameter S is zero, which implies no correlation between the phase angle and spatial one. However, in the incoherent state with $R = 0$ for $p < p_c$ the S shows finite value, which means there is some correlation between the phase and spatial angle. Moreover, the S for $p < p_c$ shows $S = 1$ for a certain region of p , and the range of p of this region depends on

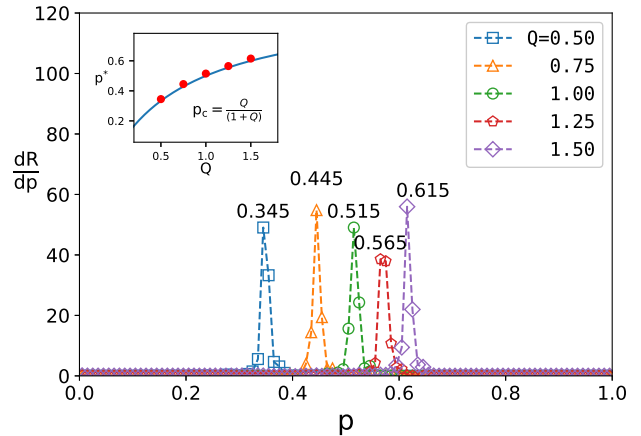


FIG. 2. (Color Online) The first derivative of R over p , dR/dp , is shown as a function of p for various values of Q , where the value of p at which dR/dp reaches the maximum value is called as p^* . Inset: p^* vs. Q is shown, where the blue solid line is the theoretical prediction given by $p_c = Q/(1+Q)$, and the value of p^* is consistent with the prediction. The system size is $N = 800$ and $J = 0.8$, and the data have been averaged over 10 samples.

the value of J as shown in Fig. 1 (b): The range gets wider as J increases.

To pin down the threshold p_c , we now estimate it numerically. We measure the value of p at which the first derivative dR/dp shows the maximum. Figure 2 shows the behavior of dR/dp as a function of p for various values of Q , where the value of p at which the dR/dp reaches the maximum is called as p^* . The inset of Fig. 2 shows p^* as a function of Q , which shows a good consistency with the theoretical prediction $p_c = Q/(1+Q)$ (see Sec. IV).

IV. LINEAR STABILITY OF THE FULLY SYNCHRONIZED STATE ($R = 1$)

In this section, we investigate the linear stability of the fully synchronized state with $R = 1$. Let a fully synchronized state have a common phase $\theta_i = \theta_s$ for all i . In order to examine its linear stability, we consider a slightly perturbed situation such as $\theta_i = \theta_s + \phi_i$ with small perturbation ϕ_i for all i . For this setting, Eq. (4) is linearized to

$$\dot{\phi}_i = \frac{1}{N} \sum_{j \neq i} \frac{K_{ij}}{r_{ij}} (\phi_j - \phi_i). \quad (8)$$

Separating the summation according to the values of K_{ij} , we rewrite Eq. (8) as

$$\dot{\phi}_i = \frac{1}{N} \left(K_p \sum_{j \in C_p(i)} \frac{1}{r_{ij}} (\phi_j - \phi_i) + K_n \sum_{j \in C_n(i)} \frac{1}{r_{ij}} (\phi_j - \phi_i) \right), \quad (9)$$

where $C_p(i)$ is the collection of j having $K_{ij} = K_p$ and $C_n(i)$ is that for $K_{ij} = K_n$, respectively.

We here note that K_{ij} is not included in the spatial dynamics [see Eq. (5)]. Thus, for a fixed i , the fraction of such j 's giving $K_{ij} = K_p$ in the total N would be approximately p , where the deviation is expected to decrease as N increases. Similarly, that for $K_{ij} = K_n$ is given by $(1 - p)$. This consideration motivates us to replace $\sum_{j \in C_p(i)}$ and $\sum_{j \in C_n(i)}$ with $p \sum_{j(\neq i)}$ and $(1 - p) \sum_{j(\neq i)}$, respectively, in Eq. (9) when N is large enough. Therefore, for large N , Eq. (9) can be cast into

$$\dot{\phi}_i = \langle K_{ij} \rangle \frac{1}{N} \sum_{j \neq i} \frac{1}{r_{ij}} (\phi_j - \phi_i). \quad (10)$$

where $\langle K_{ij} \rangle \equiv pK_p + (1 - p)K_n$ is the average of K_{ij} for the two-peak distribution $h(K_{ij})$.

Introducing $m_{ij} = -1/(Nr_{ij})$ for $i \neq j$ and $m_{ii} = -\sum_{j \neq i} m_{ij}$, one writes Eq. (10) as

$$\dot{\phi}_i = -\langle K_{ij} \rangle \sum_{j=1}^N m_{ij} \phi_j. \quad (11)$$

Interestingly, matrix $m = \{m_{ij}\}$ is positive-definite for large N as follows. It holds $|m_{ij}| \sim \mathcal{O}(1/\sqrt{N})$ for off-diagonal terms. This is based on the numerical observation that all swarmalators reside in the 2-dimensional spatial region of $\mathcal{O}(1)$ -area and there is no concentration of them. Thus, $r_{ij} \sim 1/\sqrt{N}$ holds, from which $|m_{ij}| \sim \mathcal{O}(1/\sqrt{N})$ follows. It also follows that $m_{ii} = -\sum_{j \neq i} m_{ij} \sim \mathcal{O}(\sqrt{N})$. Then, as N increases, $m = \{m_{ij}\}$ approaches $\bar{m} = \{\bar{m}_{ij}\}$ that is given by

$$\bar{m}_{ij} = \delta_{ij} \bar{m}_i, \quad (12)$$

where δ_{ij} is the Kronecker delta that assigns 1 when $i = j$ while 0 otherwise. The matrix \bar{m} is positive-definite because $\bar{m}_i \equiv \lim_{N \rightarrow \infty} m_{ii} > 0$. Therefore, m is also positive-definite for sufficiently large N .

When the positive-definiteness of m is considered in Eq. (11), one knows that the sign of $\langle K_{ij} \rangle$ determines whether ϕ_i will decay or not. This is because every eigenvalue of positive-definite matrix is positive. Thus, ϕ_i decays when $\langle K_{ij} \rangle > 0$, otherwise grows when $\langle K_{ij} \rangle < 0$. Since $Q \equiv -K_n/K_p$, it reads that $\langle K_{ij} \rangle = K_p(p + (p - 1)Q)$. Therefore, $\langle K_{ij} \rangle > 0$ corresponds to $p > Q/(1 + Q)$ and $\langle K_{ij} \rangle < 0$ does $p < Q/(1 + Q)$, which leads to

$$p_c = Q/(1 + Q). \quad (13)$$

For $Q = 1.25$, used for the numerical data shown in Figs. 1 and 2, Eq. (13) gives $p_c = 5/9 = 0.55\dots$. The deviation from the numerical value $p_c \approx 0.6$ in the figures is supposed to be a finite N effect. Note $p_c \approx 0.565$ of Fig. 2 for $N = 800$ is closer to the prediction $p_c = 5/9$ than the one of Fig. 1 for $N = 200$. It is interesting that the threshold value shown in Eq. (13) is equivalent to that for the mean-field XY-type oscillators with random coupling disorder [18]. This means that the spatial dynamics in the system does not change the threshold value of the phase transition from the incoherent state to the fully synchronized one.

The crucial step of our argument above is the use of $\sum_{j \in C_p(i)} = p \sum_{j(\neq i)}$ and $\sum_{j \in C_n(i)} = (1 - p) \sum_{j(\neq i)}$ to write Eq. (10). We here remark this is basically an annealed approximation. In fact, K_{ij} is quenched by definition in the model and has never been treated in an annealed way in the numerical work. Thus the consistency between Eq. (13) and its numerical counterpart is interesting. Equation (5) gives a clue to understanding how the quenched K_{ij} works as if annealed. The spatial dynamics governed by Eq. (5) is indifferent to K_{ij} . Based on this, one may expect the distribution of K_{ij} for given i has no position-dependence, i.e., the fractions for K_p and K_n are, respectively, p and $(1 - p)$ independent of position. This results in the annealed average of phase dynamics in Eq. (4). The consistency between the numerical data and the annealed average, even in the presence of quenched K_{ij} , means that the oscillators move to the proper places. That is, the effective annealing of K_{ij} to $\langle K_{ij} \rangle$ is a characteristic property of swarmalator that can move.

We also examine that the sign of $\langle K_{ij} \rangle$ always governs the onset of sync state in further numerical study using other $h(K_{ij})$ distributions. These observations suggest that the annealed approximation could be generally available. We remark that the effect annealing requiring proper locations of swarmalators is considered for long-term states after rapidly varying transient period.

V. NON-STATIONARY STATES IN THE INCOHERENT REGIME ($R = 0$)

In this section, we investigate the incoherent state ($R = 0$) further. In particular, we pay attention to the possibility of the nonstationary states such as the active phase wave (APW) state and the splintered phase wave (SPW) state found in Ref. [1]. Therein, the all coupling strength among the oscillators was chosen as the negative one with no disorder like $K_{ij} = K$, which corresponds to $p = 0$ in the current study. We note that, in Ref. [1], various long-term states such as async state, APW state, SPW state, and static phase wave state were found depending on the strength of the negative coupling in the phase dynamics. Especially, APW state and SPW one are the nonstationary states where the oscillators are not static in both phase and space. It is thus interesting

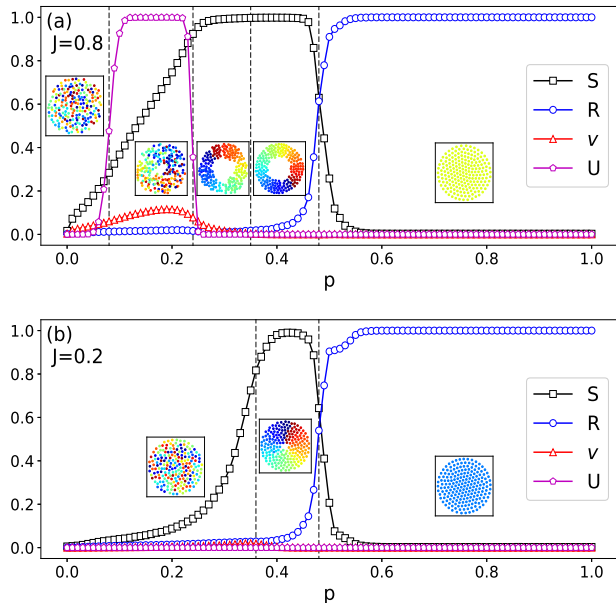


FIG. 3. (Color Online) Behavior of S , R , V , and U is shown as a function of p for (a) $J = 0.8$ and (b) $J = 0.2$. Snapshots for the corresponding regime are also shown in the insets. Parameters: $N = 200$ and $Q = 0.8$.

whether the dynamics of Eqs. (4) and (5) with quenched disorder K_{ij} can induce such nonstationary feature. Below, we again resort to the numerical data by the same scheme used for Fig. 1.

To see the possibility of the nonstationary states for $p > 0$, we measure the following two quantities. One is the mean velocity V defined by [1, 2]

$$V = \frac{1}{N} \sum_{j=1}^N v_i, \quad (14)$$

where $v_i = \sqrt{\dot{x}_i^2 + \dot{y}_i^2}$. The mean velocity measures the nonstatic property of the state. In other words, the finite value of V means that the swarmalators move around in the plane in the long-term state. The other one is [1, 2]

$$U = \frac{N_{\text{rot}}}{N}, \quad (15)$$

where N_{rot} is the number of swarmalators circulating at least 2π , thus U represents the fraction over the total swarmalators [1, 2]. Note that the U can play as a role of the indicator for the active phase wave state [1]. Figure 3 (a) and (b) show the quantities R , S , V , and U as a function of p for $J = 0.8$ and 0.2 , respectively. As p increases from zero, we find that the phase transition occurs from the incoherent state ($R = 0$) to the fully synchronized one ($R = 1$) at a finite value of p_c , as shown in the behavior of R . Interestingly, the p_c for two different values of J is found to be same, which means the threshold does not depend on J . On the other hand, the

behavior of S , U , and V is found to differ depending on the value of J (See Fig. 3).

When $R = 0$, note that the system shows finite value of S through the splintered/static phase wave. Also, the system shows the active phase wave state for small p when J is large. This active phase wave does not occur when J is small. We find that the system shows both the stationary states and the nonstationary ones depending on p for a given value of Q and J . Especially, when J is large ($J = 0.8$), the all five long-term states that have been reported in Ref. [1] exist depending on p . It is interesting to note that the nonstationary states such as active phase wave state and splintered one also exist in the presence of the positive coupling among the swarmalators in the system ($p > 0$).

VI. MIXTURE OF RANDOM COUPLINGS

Above, we have seen that the result by random K_{ij} is comparable with that by constant $K = K_{ij}$. The long-term state patterns, including fully synchronized one, from both settings are similar for large J . It is remarkable that such analogy holds in the presence of finite fraction for negative K_{ij} that may bring about the frustration [20, 21] in the phase dynamics. This strongly suggests the annealed property conjectured for the onset of sync phase at $\langle K_{ij} \rangle = 0^+$ is also valid for non-zero $\langle K_{ij} \rangle$ cases. This motivates us to test the long-term states in the system with such quenched random couplings by mixture of different randomnesses. We are interested in whether the characters by each randomness will last or not.

Consider N_1 number of swarmalators in total N , and call them group 1 (G1). The coupling strength K_{ij} , therein, is assigned with 1 for probability p_1 or -1 for $1 - p_1$. Next, consider the other group, G2, of $N_2 (= N - N_1)$ swarmalators, where $K_{ij} = \pm 1$ is similarly assigned using probability p_2 . We also consider coupling between the swarmalators in both groups as assigning 1 to K_{ij} for probability p_m or -1 for $1 - p_m$. Below, we use $p_m = 0$ only so as to allow the largest chance for frustration mediated by the pairs belonging to both groups. When $(N_1, p_1) = (100, 1)$ and $(N_2, p_2) = (100, 0)$, one may expect sync disc in G1 and APW in G2 if the frustration by the negative coupling between the groups does not overwhelms each characters. Note the average coupling in G2, $\langle K_{ij} \rangle_2 = -1$, is in the region for APW in the phase diagram reported in Ref. [1]. We obtained numerical data with time unit $dt = 0.01$ and consider 2×10^5 time steps.

Figure 4(a) shows the numerical result. There appear two patterns; one is a slightly deformed sync disc while the other is U-shaped one. We have examined the former vibrates a little (not demonstrated here) and the latter is an active phase state. The inset is the trajectory of a swarm in the U-shape. Since it sweeps the region while changing the phase, we name the state deformed APW

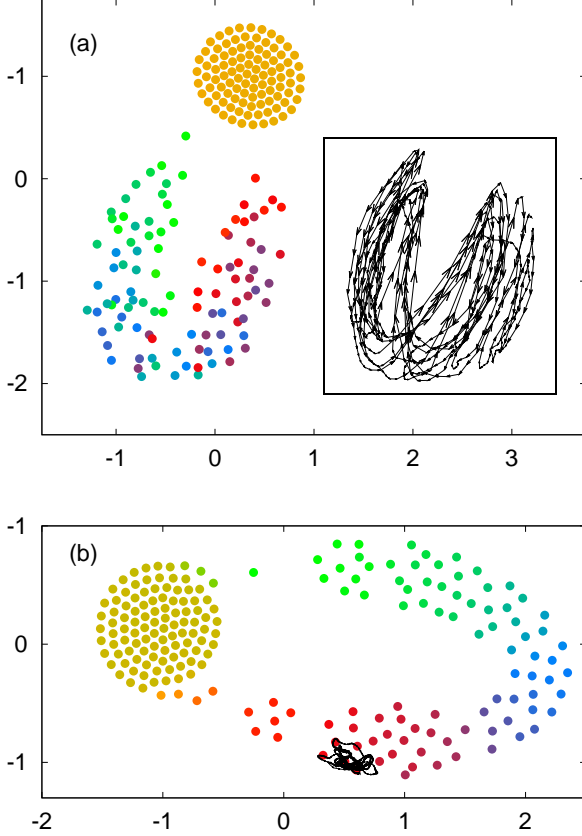


FIG. 4. (Color Online) (a) Long-term state pattern for $N_1 = N_2 = 100$, $p_1 = 1$, $p_2 = 0$, $p_m = 0$, and $J = 1$. Inset is the trajectory of an arbitrarily chosen swarmalator in the U-shaped region, which sweeps the region. (b) Long-term state pattern for the same setting used in (a) except $p_2 = 0.4$. The black solid curve is the trajectory of a swarmalator localized there.

(dAPW). It is interesting to note that this reminds us the “chimera state” observed in the oscillators with identical frequency [22–25]: Partial group of the swarmalators in the system exhibits the sync cluster, but the other group of the swarmalators do not join the sync cluster, showing the U-shape APW.

We vary N_1 to see a possible change in pattern. One easily see the distance between sync disc and dAPW increases when compares Figs. 4(a) and 5(a). We also see the sync disc becomes more circular and static when the distance increases. We next test whether a sync disc by $p_1 < 1$ in G1 only system ($N_2 = 0$) will still last after G2 is involved ($N_2 > 0$). The interest is a validity of the annealed approximation of K_{ij} in G1. Figure 5(b) is the result for $p_1 = 0.7$, which is also composed of sync disc and dAPW. The sync disc is almost circular and static with enough separation from the dAPW.

We finally test whether G2 can show SPW state while G1 remains a sync disc. As splintered state appears for the negative coupling larger than that for APW, we use

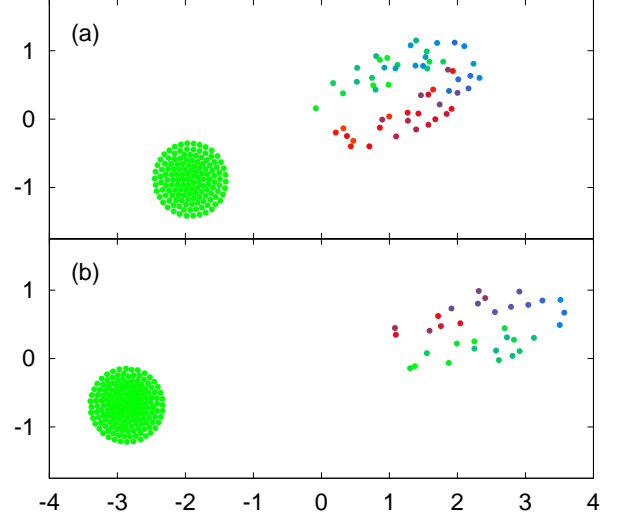


FIG. 5. (Color Online) Long-term state patterns composed of sync disc and dAPW for $N_1 = 60$, $N_2 = 140$, $p_1 = 1$, $p_2 = 0$, $p_m = 0$ in (a) and for $N_1 = 140$, $N_2 = 60$, $p_1 = 0.7$, $p_2 = 0$, $p_m = 0$ in (b).

$p_2 = 0.4$ that corresponds to $\langle K_{ij} \rangle_2 = -0.2$, the average coupling strength in G2. This value is in the region for splintered wave in the phase diagram reported in Ref. [1]. Figure 4(b) is the result when the other settings are same as those for Fig. 4(a). There still appear sync disc and U-shape. This time, the swarmalators of different colors in the U region are not mixed, different from the dAPW case. The gradual change of the swarmalators’ colors in space is a character of splintered phase wave. The black solid curve near bottom is the trajectory of a swarm, which remains near there as time goes on. As shown, it does not sweep the U region but localized in the small area while splintering. This is always the case for all swarmalators in the U region. We thus regard the U-shaped pattern as a deformed splintered phase wave (dSPW).

In the above numerical tests, the characters by each random couplings are preserved more or less in the mixed system. There apparently appear sync disc, APW, and splintered states though deformed. We here add the result is qualitatively same for the various values of p_m (not shown here), and this does not depend on the initial condition. These observations suggest that the long-term states, demonstrated in Secs IV and V, are robust not to lose their characters in the mixed system. It is remarkable that the patterns survive the maximal frustration mediated by $p_m = 0$. It is supposed that all the other superficial features are readily destabilized by the frustration due to negative couplings. A mixture with async state or of more than two groups is not tested this time. Further study on various interesting properties of the mixed deformed patterns will appear elsewhere.

VII. SUMMARY

We considered the population of swarmalators with random coupling strength, and explored how the coupling disorder affects the long-term states in the system. In particular, the possibility of the phase transition and the robustness of the state patterns are focused. To understand the long-term states observed in the system with quenched disorder of coupling strength, we consider the effective annealed approximation, which is mediated by the mobility of swarmalators. In the viewpoint of annealed couplings, the numerical observation in the quenched system is explained and, furthermore, such system of mixture of different quenched disorders is also understood.

We found that the system shows the phase transition from the incoherent state to the fully synchronized one at a certain threshold p_c , where the value of p_c is argued in the linear stability analysis of the fully synchronized state. We also found that, in the regime of the incoherent

state below the threshold, various long-term states are found to exist. Especially, the nonstationary states such as the dAPW and dSPW besides the normal APW and SPW are discovered.

All long-term states known for the bare model in [1] are realized in the system of random coupling strength. The values of average-coupling where each state appears are similar to their counterparts in the bare model. This strongly suggests the randomly quenched coupling strengths work as if annealed. The pattern by the supposed annealed coupling is so robust that the mixture of different random couplings leads to the proper combination of each deformed patterns.

VIII. ACKNOWLEDGEMENTS

This research was supported by the NRF Grant No.2021R1A2B5B01001951 and ‘Research Base Construction Fund Support Program’ funded by Jeonbuk National University in 2021 (H.H), and 2018R1D1A1B07049254 (H.K.L.).

-
- [1] K. P. O’Keeffe, H. Hong, and S. H. Strogatz, *Nature Comm.* **8** 1504 (2017).
 - [2] H. Hong, *Chaos* **28**, 103112 (2018).
 - [3] K. P. O’Keeffe, J. H. M. Evers, and T. Kolokolnikov, *Phys. Rev. E* **98**, 022203 (2018).
 - [4] A. Baris and C. Bettstetter, *IEEE Access* **8**, 218752–218764 (2020).
 - [5] H. K. Lee, K. Yeo, and H. Hong, *Chaos* **31**, 033134 (2021).
 - [6] K. O’Keeffe and C. Bettstetter, A review of swarmalators and their potential in bio-inspired computing, in *Proc. SPIE 10982, Micro- and Nanotechnology Sensors, Systems, and Applications XI* (2019) p. 10982.
 - [7] S.-Y. Ha, J. Jung, J. Kim, J. Park, and X. Zhang, *Mathematical Models and Methods in Applied Sciences* **29**, 2271–2320 (2019).
 - [8] A. Barciś, M. Barciś, and C. Bettstetter, Robots that sync and swarm: A proof of concept in *ros 2* (IEEE, 2019).
 - [9] T. A. McLennan-Smith, D. O. Roberts, and H. S. Sidhu, *Phys. Rev. E* **102**, 032607 (2020).
 - [10] J. U. F. Lizarraga and M. A. M. de Aguiar, *Chaos* **30**, 053112 (2020).
 - [11] F. Jimenez-Morales, *Phys. Rev. E* **101**, 062202 (2020).
 - [12] F. H. Martini, *Anatomy and Physiology* (Pearson Education, Inc., 2007) p. 288.
 - [13] J. J. Hopfield, *Proc. Natl. Acad. Sci. U.S.A.* **79**, 2554 (1982).
 - [14] I. Aihara, H. Kitahata, K. Yoshikawa, and K. Aihara, *Artificial Life and Robotics* **12**, 29 (2008).
 - [15] S. F. Edwards and P.W. Anderson, *Journal of Physics F: Metal Physics* **5**, 965 (1975).
 - [16] D. Sherrington and S. Kirkpatrick, *Phys. Rev. Lett.* **35**, 1792 (1975).
 - [17] H. E. Stanley, *Introduction to Phase Transitions and Critical Phenomena* (Oxford University Press, New York, 1971).
 - [18] H. Hong and E. A. Martens (in preparation).
 - [19] Y. Kuramoto, *Chemical Oscillations, Waves, and Turbulence* (Springer, Berlin, 1984).
 - [20] J. Vannimenus and G. Toulouse, *G., J. Phys. C.* **10**, L537 (1977).
 - [21] G. Toulouse, The frustration model, in *Modern Trends in the Theory of Condensed Matter* edited by A. Pekalski and J. Przystawa. *Lecture Notes in Physics* **115** (Springer, Berlin, 1980), p. 195.
 - [22] Y. Kuramoto and D. Battogtokh, *Nonlinear Phenom. Complex Syst.* **5**, 380 (2002).
 - [23] Y. Kuramoto, Where Do We Go from Here?, in *Nonlinear Dynamics and Chaos* edited by S. J. Hogan, A. R. Champneys, B. Krauskopf, M. di Bernardo, R.E. Wilson, H. M. Osinga, and M. E. Homer (Institute of Physics, Bristol, U.K., 2003), p. 209.
 - [24] S.I. Shima and Y. Kuramoto, *Phys. Rev. E* **69**, 036213 (2004).
 - [25] D. M. Abrams and S. H. Strogatz, *Phys. Rev. Lett.* **93**, 174102 (2004).